GAIN, IMPEDANCE MEASUREMENTS AND DIELECTRIC LOADING OF GROUND PENETRATING RADAR (GPR) ANTENNAS USING A WATERTANK TESTING FACILITY

Aaron A. Chong, Christopher J. Leat and Glen F. Stickley

Department of Computer Science and Electrical Engineering
The University of Queensland, Qld 4072, AUSTRALIA
and the
Cooperative Research Centre for Sensor Signal and Information Processing (CSSIP)
The University of Queensland, Qld 4072, AUSTRALIA
chonga@cssip.uq.edu.au, leat@cssip.uq.edu.au and stickley@cssip.uq.edu.au

ABSTRACT

The design and testing of suitable GPR antennas to be used in the field is both an arduous and challenging task. Presented here is a watertank testing facility incorporating a method of measuring gain and impedance of scaled-down models of prospective GPR antennas. A vertical ground plane is placed in a watertank measuring 1200mm×600mm×600mm. A monopole version of the test antenna is connected to a 150mm square plate which fits exactly into the ground plane. Underwater and air probes are placed in a semi-circular fashion on the vertical conducting ground plane around the square plate at radii of 150mm and 300mm respectively. Results are presented as gain and impedance plots for a monopole test antenna with two different water levels; 0mm and 5mm below the base of the test antenna. Results for a salty solution and Isopropylalcohol dielectrically loaded, cavity backed, slot bowtie antenna are also given. The results show the sudden change in electrical length that occurs near a half-space surface, lateral wave phenomena as an air gap appears between the antenna's base and the water's surface as well as improved fractional bandwidth through dielectric loading.

Key words: Watertank, Vertical Ground Plane, Bowtie Antenna, Dielectric Loading, Salty Solution, Isopropylalcohol.

INTRODUCTION

A photograph showing the watertank used to facilitate the characterising of GPR antennas in a controlled environment is shown in figure 1. It has physical dimensions of 1200mm×600mm×600mm. It is a useful tool for validating modelled results as well as empirically determining the characteristics of a particular antenna using scale models [Leat,(1998)]. Alternate probes are placed on opposite sides of a semi-circle on the vertical conducting ground plane in 15° degree intervals to create greater distance separations between the probes and minimise the cross-coupling effects between them. The water-tight cavity of the watertank is shown in figure 2(a). It forms the backbone of the watertank and is attached to the back of the vertical ground plane. The water-tight cavity keeps the connectors dry and by having a mounting bracket in place, all the SMA connectors and the antenna feed-point can be easily accessed and convenient measuring positions are easily located. An underwater probe in the form of an SMA paneljack is shown in figure 2(b). The length of the teflon enclosed dielectric paneljack is stripped and its overall length reduced to 6mm. The air probes are also SMA paneljacks but with a thin wire extension on them to extend their overall length to 52mm. Figure 3 shows the model test antenna to be used in the watertank. The 150mm square plate is made of aluminium and the bowtie is made of copper. The bowtie is soldered on to a SMA paneljack which acts as the

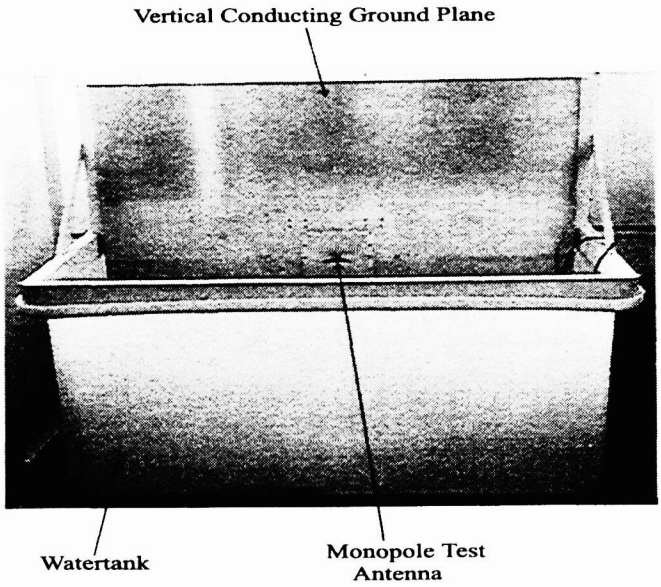

Figure 1: Photo showing the watertank

In *Eighth Intl. Conference on Ground Penetrating Radar*, David A. Noon, Glen F. Stickley, Dennis Longstaff, Editors, SPIE Vol. 4084 (2000) • 0277-786X/00/$15.00

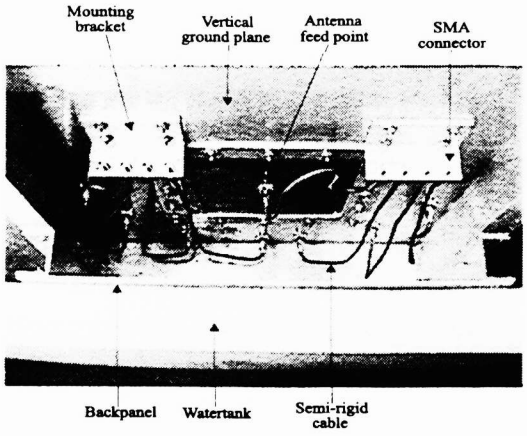

(a)

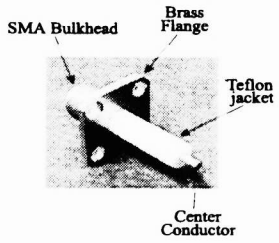

(b)

Figure 2: (a) Water-tight cavity of the watertank (b) SMA paneljack

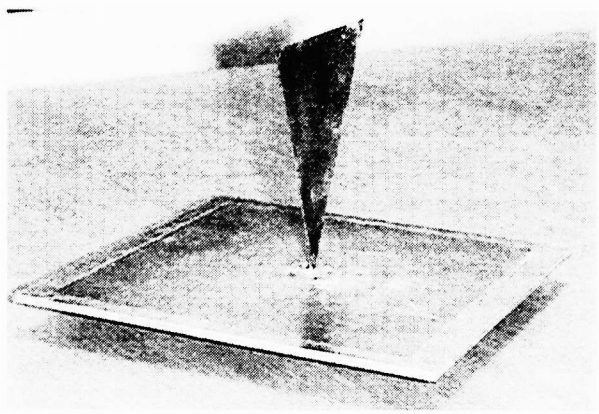

Figure 3: Photo of monopole bowtie test antenna

feed point of the antenna and protrudes through the back of the square plate as a connector to the HP-8510c network analyser.

PROBE CALIBRATION

Probe to probe calibration was carried out using one probe as a transmitting antenna and another probe as the receiving antenna. 15°, 30°and 45° angle separations were used to measure the S_{12} coupling values between the probes. Probe to probe calibration was done for both the underwater as well as air probes. The 0° underwater and air probes are directly underneath and above the antenna feed point at 150mm and 300mm respectively. Figure 4(a) shows the c values or the y-

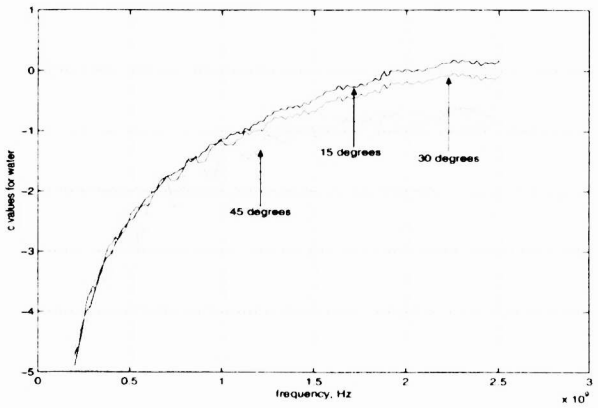

(a)

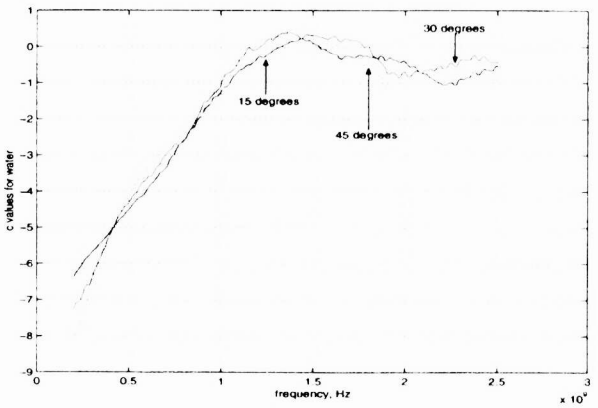

(b)

Figure 4: Graph of (a) c values versus frequency for water and (b) c values versus frequency for air

intercepts for water from 200MHz to 2.5GHz at 15°, 30°and 45° angle separations. The c values come from the Friis equation cast in the form; $y = 2x + c$, where $y \equiv log\left(\frac{P_r}{P_t}\right)$, $x \equiv log\left(\frac{\lambda}{4\pi r}\right)$ and $c \equiv 2logG_{pp}$. The c values mutual agreement give us confidence that the calibration model is performing to expectations. The oscillations present in the curve for

45° angular separation in Figure 4(a) occur because there is an intermediate probe in the middle of any two underwater probes with a 45° angular distance. The intermediate probe acts as a scattering device which causes multipath interference and prevents clear passage of waves travelling from the transmitting to the receiving probes. Figure 4(b) gives the corresponding c values for the air probes.

Using G_{pp}, the maximum effective area of the probes can be found using $A_{em} = \frac{\lambda^2}{8\pi} G_{pp}$ [Balanis,(1997)] (adjusted for a monopole). From this, we can get the electric field strength measured by the probes as;

$$| E | = \sqrt{\frac{S_{12} Re(Y) \eta}{4(1 - | \Gamma^2 |) A_{em}}} \quad (1)$$

where $Y = \frac{1}{Z}$ is the input admittance of the antenna, S_{12} are the coupling values, η is the intrinsic impedance of the medium, Γ is the reflection coefficient and it is assumed that the antenna is driven by a 1 volt source.

GAIN MEASUREMENT

For an antenna over a half-space and either medium being dissipative, the antenna gain is given as [Smith,(1984)]

$$G = \frac{4\pi r^2 | E |^2 e^{2\alpha r}}{2\eta P_{in}} \quad (2)$$

where the exponential term ($e^{2\alpha r}$) compensates the gain of the antenna for propagation losses in the water. We know that

$$P_t = (1 - | \Gamma |^2) P_{in} = \frac{V^2 Re(Y)}{2} \quad (3)$$

so by combining equations (2) and (3) we can get the gain formula for the test antenna as

$$G(\theta, \phi) = (1 - \Gamma^2) \frac{4\pi e^{2\alpha r} | E(r, \theta, \phi) |^2 r^2 \sqrt{\epsilon'}}{Re(Y) \eta_o} \quad (4)$$

where η_o is the intrinsic impedance of free-space, reflection coefficient $\Gamma = \frac{Z - Z_o}{Z + Z_o}$, ϵ' used here is the real part of the complex relative permittivity, E is the field measured assuming a 1 volt peak driving source and r is the radial distance from the antenna feed-point to the probes [King & Smith, (1981)]. Given the intrinsic impedance of the propagating medium as;

$$\eta = \frac{\eta_o}{\sqrt{\epsilon'_r}} \quad (5)$$

so by substituting equations (5) and (1) into equation (4) we obtain a simplified version of the gain formula for the test antenna;

$$G(\theta, \phi) = \frac{\pi e^{2\alpha r} S_{12} r^2}{A_{em}} \quad (6)$$

as seen by the underwater probes and

$$G(\theta, \phi) = \frac{\pi S_{12} r^2}{A_{em}} \quad (7)$$

as seen by the probes in the air.

MEASUREMENT OF A 60° BOWTIE ANTENNA

Figures 5(a) and 5(b) show the measured and computed resistance and reactance of the monopole bowtie model for 0mm and 2mm water levels respectively. The measured results agree well with the computed results of a Method of Moment model (MoM) [Leat,(1998)]. The values do not match exactly because small height variations cannot be accurately measured in the watertank. The MoM model does not consider variables such as the meniscus of the water and thickness of the copper which the test antenna is made. Figures 6(a) and (b) show the measured gain for the underwater and air probes for an unshielded monopole bowtie at 0mm water level. The nulls seen in the plots are due to the large electrical length of the monopole bowtie antenna when the feed point is in intimate contact with the water. The nulls in the H-plane occur when the electrical length for a wire dipole;

$$l_{elec} = n\lambda_e \quad (8)$$

where n=1,2,3.... and λ_e is the effective wavelength. As a result of this, many nulls occur since the electrical length is approximately six times longer when the feed point is in intimate contact with the water.

Figures 7(a) and (b) show the gain plots at 2mm water level. The nulls have now disappeared from the frequency range measured because the feed point of the antenna is no longer in contact with the water, which means its electrical length is not as long as before. This also emphasises how the electrical length is a step-function of the height of an antenna at a half space surface. A closer look at the 75° and 90°underwater probes in figure 7(a) shows an apparent increase in gain due to lateral wave propagation. Because the vertical distance of the 75° and 90° probes to the surface of the water is much less than that of the other probes, the energy emitted from the feed point of the antenna has a much shorter distance to travel in water, hence the 75° and 90° probes are over compensated by the ($e^{2\alpha r}$) factor of equation (2). Figure 8 shows the arrival times of the waves arriving at the underwater probes. It can be clearly seen that the waves incident upon the 75° and 90°probes arrive earlier than those for the other underwater probes. This confirms the lateral wave hypothesis.

MEASUREMENT OF A DIELECTRIC-LOADED, CAVITY-BACKED, SLOT BOWTIE ANTENNA

Daniels et. al, (1988) states that dielectric loading of antennas may improve their performance. Presented here are results which show that a dielectrically loaded, cavity backed,

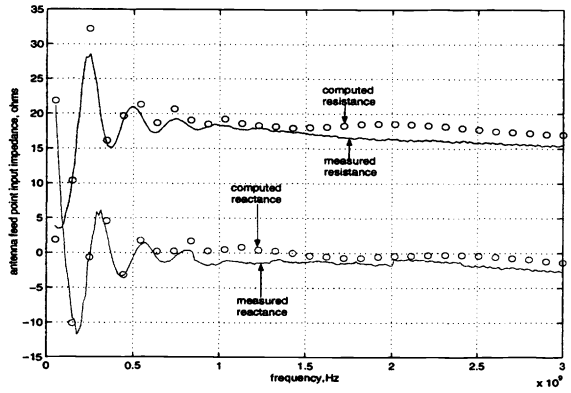

(a)

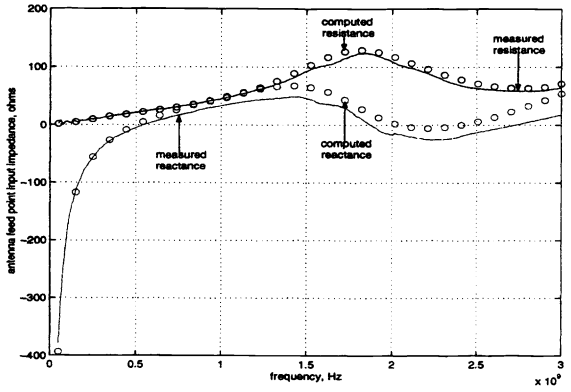

(b)

Figure 5: Measured and computed input impedance for monopole bowtie model at (a) 0mm water level and (b) 2mm water level.

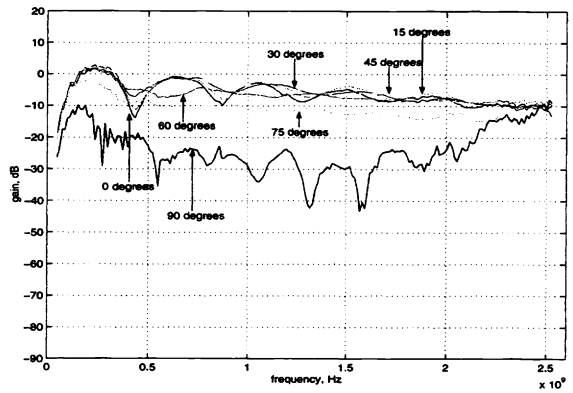

(a)

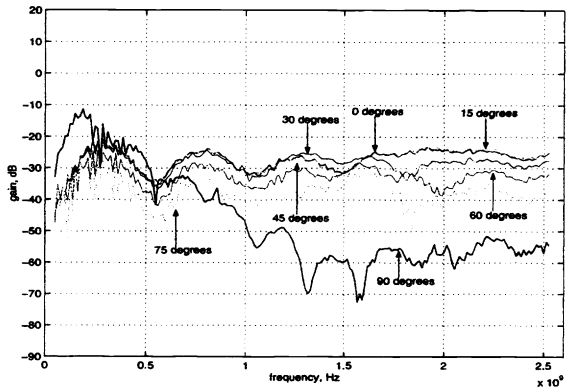

(b)

Figure 6: Gain plots of unshielded monopole bowtie for 0mm water level (a) Underwater probes (b) Air probes.

slot bowtie antenna does improve the relative bandwidth of the antenna but at the cost of reduced gain. Figure 9 shows the gain curves of such an antenna loaded with a thin salty solution. The salty solution is made by dissolving varying amounts of salt in distilled water to make the solution more lossy. Clearly seen in figure 9(a) for the underwater probes is the broadband operation from 150MHz to 600MHz. Compare this to figure 6(a) for a bowtie test antenna without disspative dielectric loading which operates from 200MHz to 500MHz. Another big difference between the loaded test antenna and the unloaded version is the reduction in gain. There is a 4dB or 5dB decrease in gain for the loaded test antenna and this is inherent in dissipatively loaded antennas. However, this is compensated by the increased relative bandwidth and the reduction in the size of the antennas through dielectric loading. Figure 10 shows the gain for a 5mm air gap introduced between the test antenna's base and the waters' surface. Again, the big difference is the reduction in gain of the dielectrically loaded modified test antenna. A thin layer of dielectric appears to have similar properties to that of the unloaded test antenna when the air gap is introduced and this is seen when figure 10(a) is compared with figure 7(a). Isopropylalcohol is another dielectric which was used to load the test antenna. Isopropylalcohol has a relatively low dielectric constant (20) compared to water (80) and it served as a good test to see whether it was a feasible dielectric with which to load GPR antennas. As can be seen from figure 11, Isopropylalcohol completely filling the cavity has a similar effect to the thin layer of salty water. The ability to control the parameters of layer thickness and conductivity has caused us to focus our efforts on the thin salty layer.

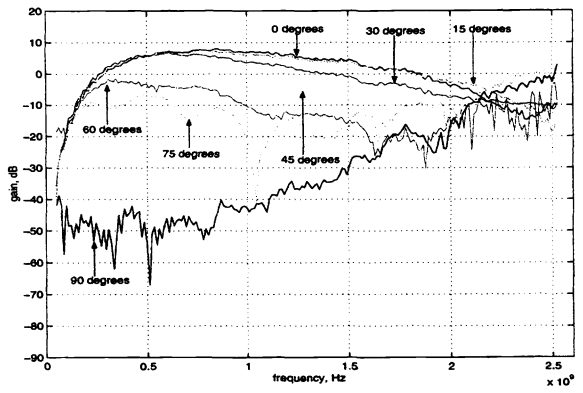

(a)

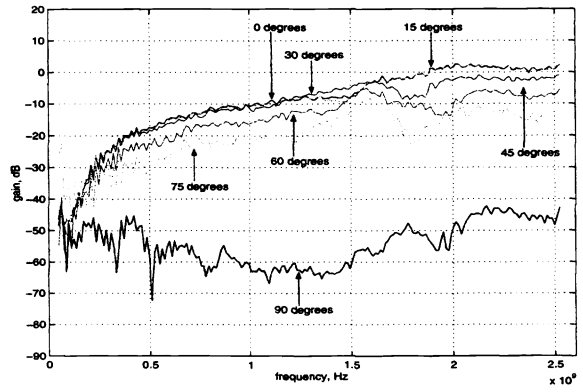

(b)

Figure 7: Gain plots of unshielded monopole bowtie for 2mm water level (a) Underwater probes (b) Air probes.

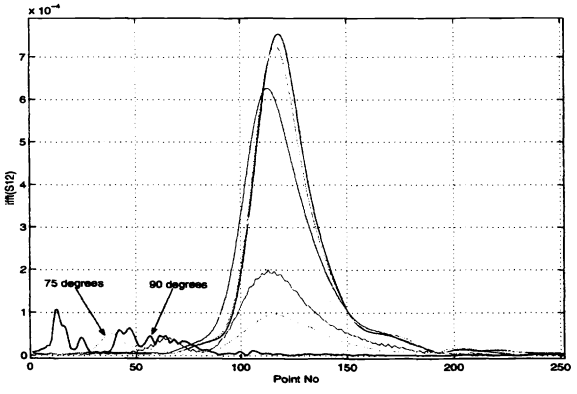

Figure 8: Inverse Fast Fourier Transform (IFFT) of S_{12} data from the unshielded monopole bowtie at 2mm water level.

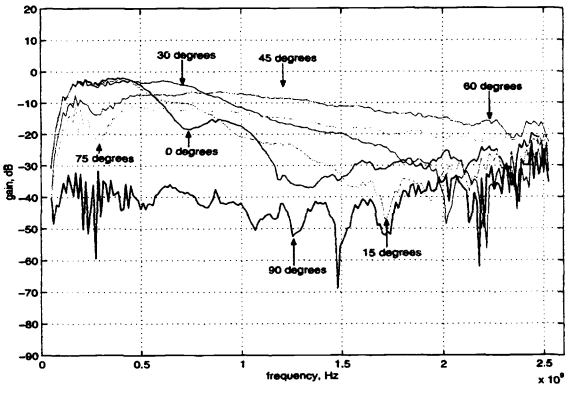

(a)

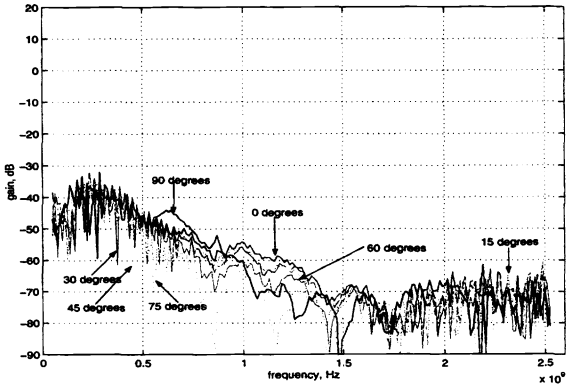

(b)

Figure 9: Gain plots for thin layer salty solution dielectric at 0mm water level (a) Underwater probes (b) Air probes.

CONCLUSIONS

Gain and impedance information which was obtained from using the watertank apparatus gives us a useful design tool for designing and constructing future GPR antennas. Dielectric loading was also shown to increase the relative bandwidth of some GPR antennas. Using a MoM model, results can be obtained numerically and then compared with the practical results from the watertank to prove feasibility and practicality of GPR antennas. The results presented here also show the sudden change in electrical length near a half-space. The work carried out here paves the way for measuring electric fields in the E-plane with minor modifications to the watertank by means of incorporating small, free moving loop probes on rails.

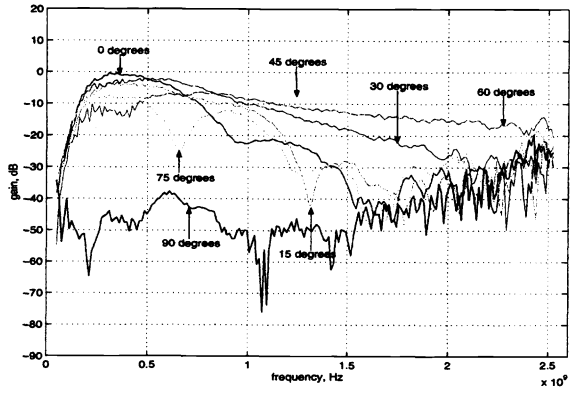

(a)

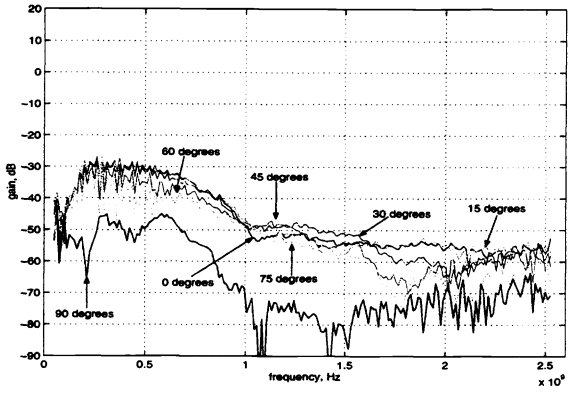

(b)

Figure 10: Gain plots for thin layer salty solution dielectric at 5mm water level (a) Underwater probes (b) Air probes.

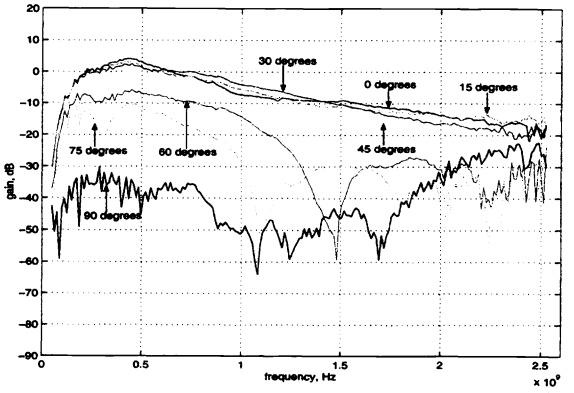

(a)

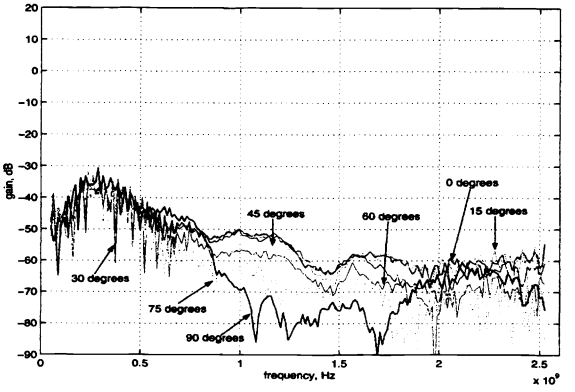

(b)

Figure 11: Gain plots for thin layer Isopropylalcohol dielectric at 0mm water level (a) Underwater probes (b) Air probes.

REFERENCES

C.A. Balanis. *Antenna Theory, Analysis and Design.* John Wiley & Sons, 1997.

R.W.P. King and G.S. Smith. *Antennas in Matter, Fundamentals, Theory and Applications.* The MIT Press, 1981.

C.J. Leat. *The Modelling and Design of GPR Antennas.* PhD thesis, University of Queensland, 1998.

G.S. Smith. Directive Properties of antennas for transmission into a material half-space. *IEEE Transactions on Antennas and Propagation,* 32(3):232-246, March 1984.

D.J. Daniels, D.J. Gunton, H.F. Scott. Introduction to Subsurface Radar. *IEE Proceedings, Vol. 135, Pt. F, No. 4, August 1988.*